# Evaluation of Nondestructive Test Methods for Length, Diameter, and Stiffness Measurements on Drilled Shafts

GLENN J. RIX, LAURENCE J. JACOBS, AND CLAY D. REICHERT

Sonic echo, sonic mobility, dynamic impedance function, and impedance log tests were used to estimate the length, diameter, low-strain stiffness, and existence of defects for two drilled shafts. An overview of the data acquisition, processing, and interpretation procedures for each test is presented. The length measurements agreed well with the design length of one shaft but underestimated the length of the second shaft, possibly because the shaft was socketed into rock. Impedance log tests provided the most accurate diameter measurements that agreed remarkably well with the diameters backcalculated from the volume of concrete. Values of the low-strain axial stiffness were nearly the same for both shafts, but were higher than the stiffnesses observed in the static load tests because of the different strain levels involved in each test.

Nondestructive integrity tests offer a cost-effective means of assessing the depth, diameter, existence of defects, and low-strain stiffness of deep foundations. These tests are frequently used as quality control tests to check for defects arising from drilling, casing, slurry, or concreting problems that could adversely affect the performance of the shaft.

The purpose of this paper is to compare results obtained using four integrity tests on two drilled shaft foundations. The shafts were part of a static load test program cosponsored by the American Society of Civil Engineers (ASCE), Association of Drilled Shaft Contractors (ADSC), Georgia Tech's School of Civil Engineering, and the Federal Highway Administration (FHWA). The primary intent of the drilled shaft load test program was to study load transfer characteristics of drilled shafts in residual soils and to evaluate methods of predicting capacity using laboratory and in situ tests.

The following sections present the essential aspects of data acquisition, processing, and interpretation for each of the four methods. Results are presented, and comparisons between the nondestructive methods and the static load tests are discussed.

## SITE DESCRIPTION AND SOIL PROPERTIES

An important criterion for the site of the load tests was that there be a sufficient thickness of residual soil to study load transfer characteristics in these soils. A site on the Georgia Tech campus where the depth to partially weathered rock (PWR) is 18–21 m (60–70 ft) was selected. The general soil profile consists of about 1 m (3 ft) of fill underlain by silty fine sands extending down to the PWR. A log from one of the soil borings at the site is shown in Figure 1. The Standard Penetration Test (SPT) blow counts generally range between 10 and 20 for the residual soils and upwards of 50 in the PWR.

A spectral analysis of surface waves (SASW) test was performed at the site to measure the shear wave velocity profile. Using the shear wave velocities, values of initial tangent shear modulus ($G_{max}$) were calculated to use in predicting the small and intermediate-strain level behavior of the shafts in axial loading. The shear wave velocity profile is presented in Table 1. Cone penetrometer, dilatometer, and pressuremeter tests were also performed at the site. The laboratory testing phase of the project includes index, consolidated-undrained ($\overline{CU}$), incremental consolidation, and resonant column/torsional shear tests.

Six drilled shafts were installed at the site, three test shafts and three reaction shafts, in a triangular pattern. All of the shafts were constructed "dry." One of the three test shafts was an "end bearing only" shaft and was not filled with concrete. The two remaining test shafts, C1 and C2, were used in this study to evaluate the four nondestructive test methods. Figure 2 shows a schematic illustration of the shafts. Shaft C1 was 21.4 m (70.2 ft) long with the tip in PWR, and Shaft C2 was 16.9 m (55.5 ft) long with its tip in residual soil. Both shafts had a nominal diameter of 762 mm (30 in.). Shafts C1 and C2 and one of the 1220-mm (48-in.) diameter reaction shafts were fully instrumented. Harris (*1*) provides a complete description of the load test program and results.

## NONDESTRUCTIVE TEST METHODS AND RESULTS

The four nondestructive methods that were used in this study are the (a) sonic echo, (b) sonic mobility, (c) dynamic impedance function, and (d) impedance log tests. All four methods share the same basic equipment configuration and test procedure in the field. This configuration is shown in Figure 3. A transient force is applied to the top of the shaft by an instrumented 5.4-kg (12-lb) sledge hammer. The force applied to the shaft is measured by a dynamic force transducer in the face of the hammer. The response of the pile to the impact is measured by a piezoelectric accelerometer attached to the shaft with mounting wax. Both force and acceleration are recorded by a Fast Fourier Transform (FFT) analyzer capable of processing data in either the time or frequency domain. The four methods differ in the way that the force and accel-

School of Civil Engineering, Georgia Institute of Technology, Atlanta, Ga. 30332–0355.

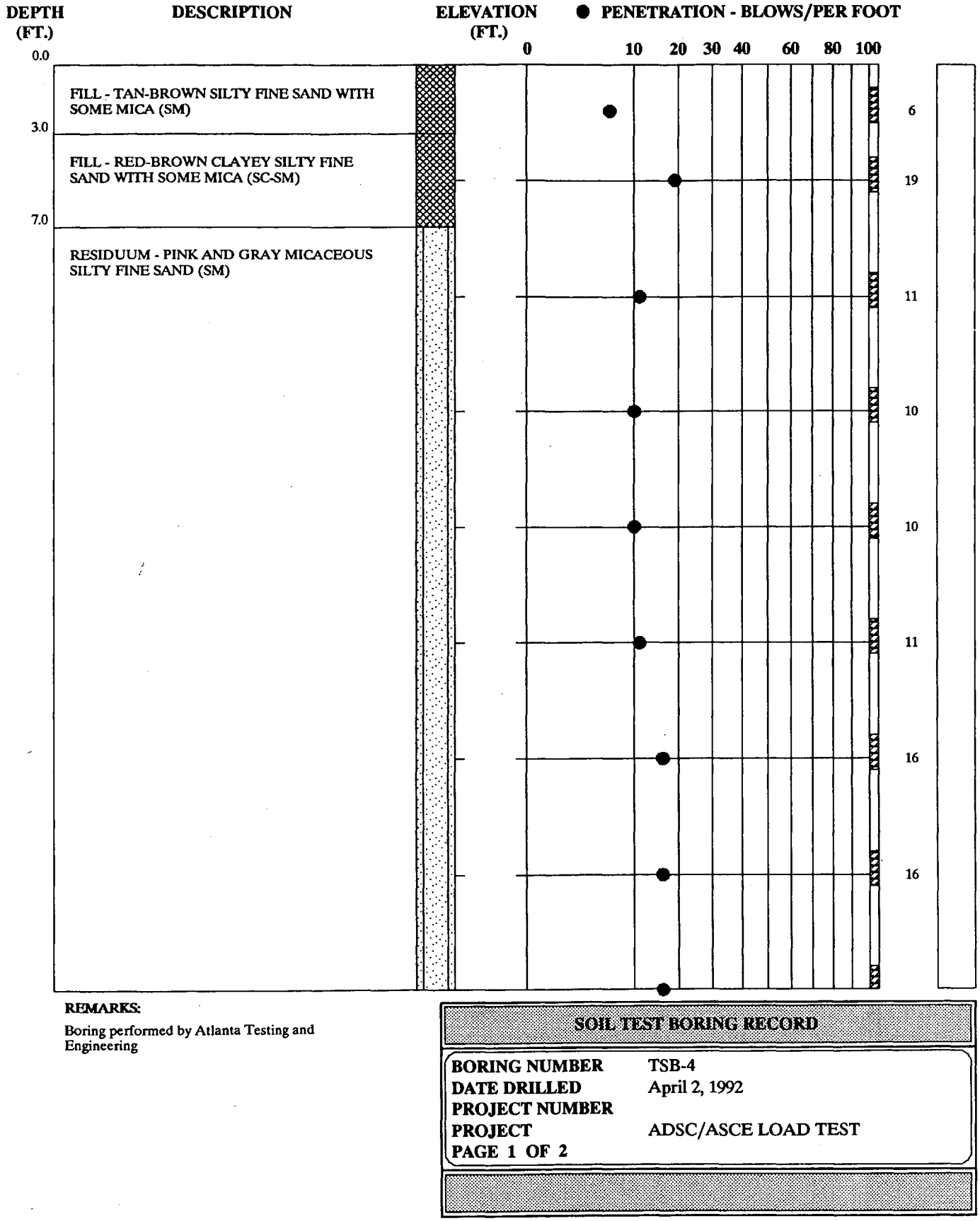


**FIGURE 1** Boring log from load test site (*continued on next page*).

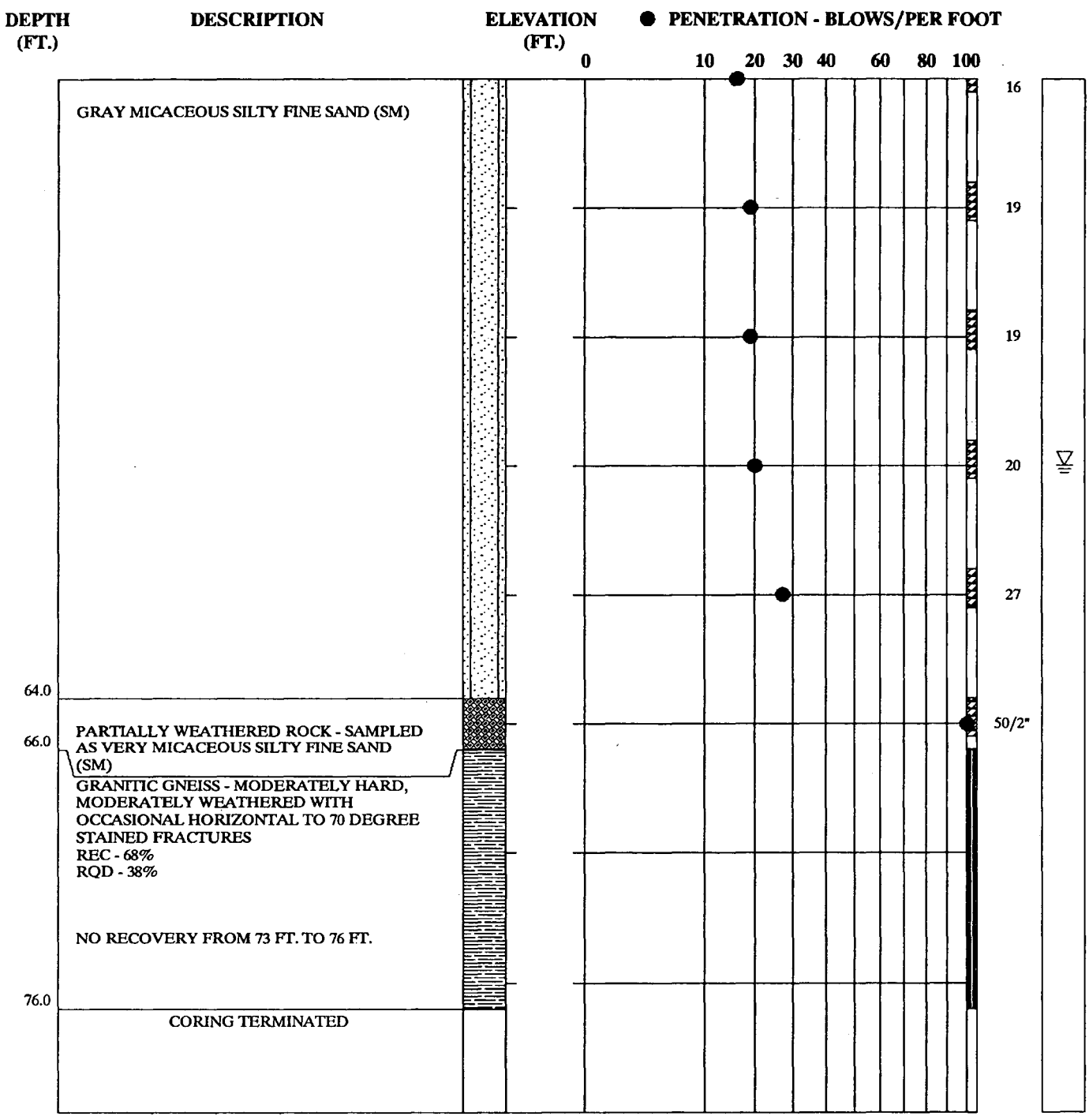


**REMARKS:**

Boring performed by Atlanta Testing and Engineering

**SOIL TEST BORING RECORD**

| | |
|---|---|
| **BORING NUMBER** | TSB-4 |
| **DATE DRILLED** | April 2, 1992 |
| **PROJECT NUMBER** | |
| **PROJECT** | ADSC/ASCE LOAD TEST |
| **PAGE 2 OF 2** | |

**FIGURE 1** (*continued*)

**TABLE 1 Summary of Spectral Analysis of Surface Wave Test Results**

| Layer No. | Layer Thickness (m) | Layer Depth (m) | Shear Wave Velocity (m/sec) |
|---|---|---|---|
| 1 | 3.05 | 3.05 | 168 |
| 2 | 3.05 | 6.10 | 240 |
| 3 | 3.05 | 9.15 | 284 |
| 4 | 3.05 | 12.20 | 323 |
| 5 | 3.05 | 15.25 | 356 |
| 6 | 6.10 | 21.35 | 387 |

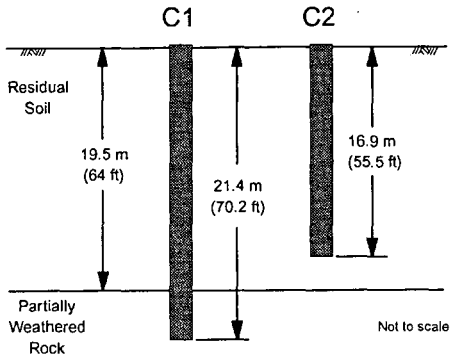


**FIGURE 2 Schematic illustration of drilled shafts.**

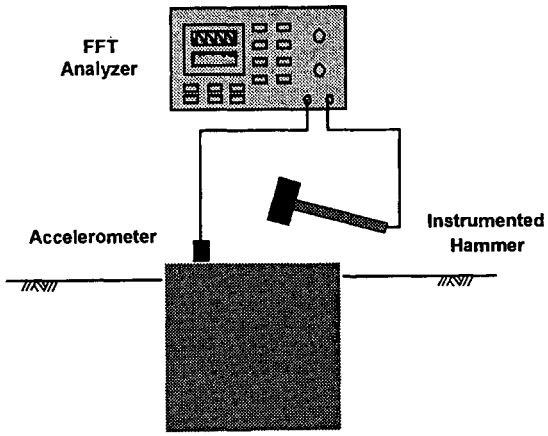


**FIGURE 3 Configuration of equipment used for nondestructive tests.**

eration time histories are processed. The following sections summarize the methods of interpretation and present the results of each test method for Shaft C2.

## Sonic Echo

Conceptually, the sonic echo method is the simplest of the four. The end of the shaft and any defects that exist along its length cause reflections of the seismic waves as they propagate downward through the shaft. By observing the time required for these reflections to return to the top of the shaft, the depth to the reflector can be determined:

$$z = \frac{v_c \cdot \Delta t}{2} \quad (1)$$

where

$z$ = depth to the reflector (a defect or the bottom of the shaft),
$v_c$ = compression wave velocity in concrete, and
$\Delta t$ = travel time of the reflected wave.

Because $\Delta t$ is a two-way travel time, the numerator in Equation 1 must be divided by two. Hearne et al. (*1*), Stain (*2*), and Olson and Wright (*4*) provide complete descriptions of the method.

The acceleration time history recorded at the top of Shaft C2 is shown in Figure 4. There was a clearly-identified reflection that occurred 9.47 msec after the initial impact. The compression wave velocity of the concrete measured on 15- × 30-cm (6- × 12-in.) test cylinders was equal to 3700 m/sec (12,130 ft/sec). Using the observed travel time and compression wave velocity, the depth to the reflector was calculated to be 17.5 m (57.4 ft). The depth agreed well with the design length of 16.9 m (55.5 ft). No other reflections could be identified in the acceleration record. Although very simple to apply, the disadvantage of the sonic echo method is that the diameter and low-strain axial stiffness of the shaft cannot be determined.

## Sonic Mobility

In the sonic mobility method, the force and acceleration time histories are transformed to the frequency domain using the FFT analyzer. The results are the spectra, $P(f)$ and $A(f)$, of

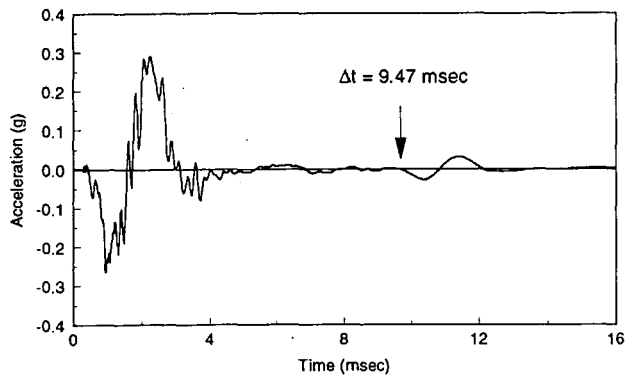


**FIGURE 4 Acceleration time history observed at the top of Shaft C2.**

the force and acceleration, respectively. The mobility is a frequency response function defined as the particle velocity observed at the top of the shaft normalized by the force:

$$\text{Mobility} \equiv \frac{V(f)}{P(f)} = \frac{A(f)}{i\omega P(f)} \tag{2}$$

where

$V(f)$ = the particle velocity spectrum,
$\omega = 2\pi f$ is the circular frequency, and
$i = \sqrt{-1}$.

The particle velocity spectrum is obtained by integrating the particle acceleration spectrum in the frequency domain as shown in the right-hand term of Equation 2. The mobility is a complex quantity, but typically only the magnitude is plotted. Figure 5 shows the mobility curve measured for Shaft C2. The shaft length and depth to defects, average diameter, and stiffness are determined from the curve using the following interpretive procedures (*3,5*).

The length of the shaft and the depth to any defects are determined from the spacing between peaks, $\Delta f$:

$$z = \frac{v_c}{2 \cdot \Delta f} \tag{3}$$

In Figure 5, the spacing between adjacent peaks is 107.5 Hz. This corresponds to a shaft length of 17.2 m (56.4 ft), which also agrees well with the design length of 16.9 m (55.5 ft). Defects in the shaft would appear as more-widely-spaced peaks with larger amplitudes. No other peaks are evident in Figure 5, indicating that the shaft has no major defects.

The average impedance of the shaft can be determined using the average value of the mobility at higher frequencies:

$$N = \frac{1}{\rho_c \cdot A_c \cdot v_c} \tag{4}$$

where

$N$ = the average value of the mobility,
$\rho_c$ = the mass density of concrete, and
$A_c$ = the average cross-sectional area of the concrete.

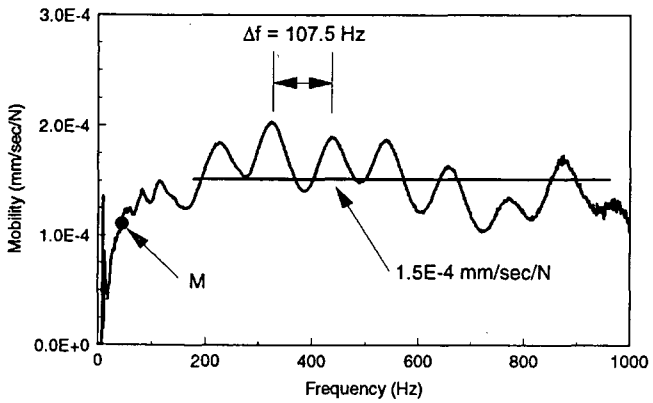


**FIGURE 5 Mobility curve for Shaft C2 showing interpretation for length, diameter, and stiffness.**

Because the mass density and compression wave velocity can be measured or assumed with little error, Equation 4 can be used to calculate the average cross-sectional area (or diameter) of the shaft. In Figure 5, the average value of the mobility from 200 to 1,000 Hz is identified by the horizontal line at $1.5 \times 10^{-4}$ mm/sec/N. Using the measured $v_c$ and a measured unit weight of 23.5 kN/m³ (150 pcf), the average diameter of the shaft was 979 mm (38.5 in.).

The low-strain stiffness was calculated from the slope of the initial portion of the mobility plot:

$$K_{\text{mob}} = \frac{2\pi f_M}{\left|\frac{V(f)}{P(f)}\right|_M} \tag{5}$$

where $K_{\text{mob}}$ is the low-strain stiffness, $f_M$ is the frequency of a point on the initial slope of the curve, and the term in the denominator is the magnitude of the mobility at that frequency. The low-strain stiffness varied depending on the frequency used in Equation 5. For Shaft C2, the stiffness varied from 2.0 to 2.7 MN/mm (11,421 to 15,420 kips/in.) when frequencies from 25 to 50 Hz were used in Equation 5.

The low-strain stiffness is often several times larger than the working load stiffness because of the difference in strain levels. For this reason, the low-strain stiffness is often used as a relative measurement. Once a typical value is established for the shafts at a site, shafts that have stiffnesses that differ significantly from the typical value can be identified as suspect.

### Dynamic Impedance Function

This approach is frequently used to predict the response of foundations to dynamic loads (*6,7*). Although it has not been widely used for integrity tests, it provides another means of calculating the dynamic stiffness of the shaft or other deep foundation. The dynamic stiffness ($K^*$) of the pile can be expressed as a complex impedance function:

$$K^* = \frac{P(f)}{U(f)} = K_r + iK_i \tag{6}$$

where $U(f)$ is the particle displacement spectrum. The real part of the complex number reflects the stiffness of the foundation system and the imaginary part reflects the damping. The complex stiffness is easily obtained from the mobility plot previously described by integrating in the frequency domain to convert the velocity to a displacement and taking the inverse:

$$K^* = \left(\frac{V(f)}{i\omega P(f)}\right)^{-1} = \left(\frac{-A(f)}{\omega^2 P(f)}\right)^{-1} \tag{7}$$

In many cases, the real part of the stiffness can be considered independent of the frequency and approaches the static stiffness at low frequencies (*7*). Figure 6 shows the real part of the complex impedance function for Shaft C2. Data at frequencies less than 20 Hz were contaminated by noise and have been removed from the plot. The average value of the stiffness between 20 and 100 Hz is 1.8 MN/mm (10,278 kips/in.).

The low-strain stiffness from the dynamic impedance function is about 10 to 30 percent lower than the stiffness from

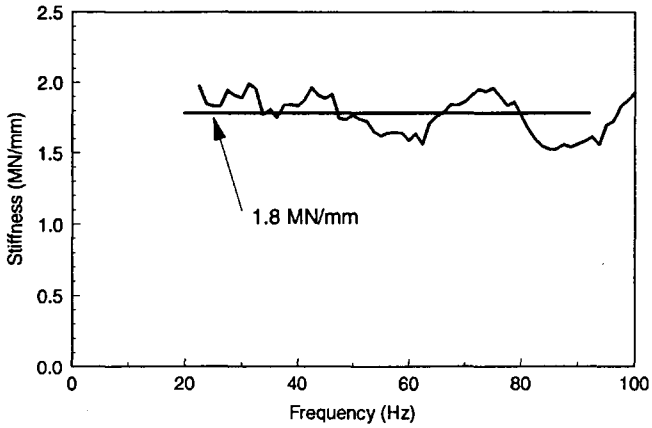


**FIGURE 6 Real part of the dynamic impedance function for Shaft C2 showing interpretation of stiffness.**

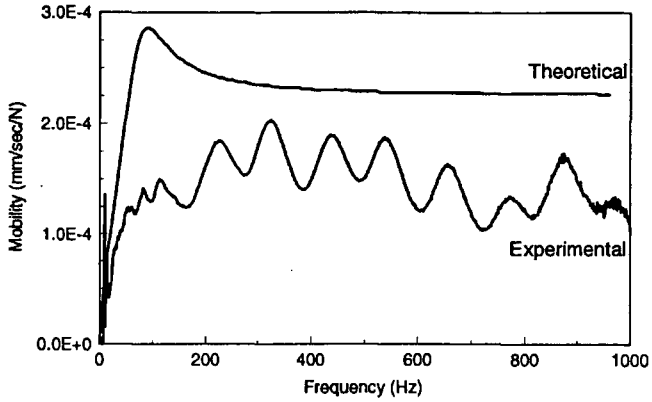


**FIGURE 7 Experimental and theoretical mobility curves for Shaft C2.**

sonic mobility measurements, depending on the frequency used in Equation 5. In the dynamic impedance function approach, the stiffness is calculated using only the real part of the complex stiffness. However, the definition of $K_{mob}$ in Equation 5 includes both the real and imaginary parts of the complex stiffness because the magnitude of the mobility is used to calculate $K_{mob}$. As a result, the definition of $K_{mob}$ includes the contribution of damping as well as stiffness. Because damping generally increases with frequency for deep foundations (*7*), $K_{mob}$ will increase with frequency and will exceed $K_r$. If one of the goals of using nondestructive tests is to estimate the low-strain static stiffness of a drilled shaft, $K_r$ provides a better estimate because the influence of damping is excluded.

### Impedance Log

The impedance log is a relatively new nondestructive testing method (*8*). The basic idea of the approach is that reflection coefficients associated with changes in impedance along the length of the shaft can be determined by processing the velocity time history observed at the top of the shaft. Using these reflection coefficients, the changes in impedance can be backcalculated.

The first step in processing the velocity time history is to isolate reflections caused by changes in impedance along the shaft by subtracting the motion at the top of the shaft due to the impact of the hammer and the soil reaction along the length of the shaft. This is performed by calculating a theoretical mobility plot for a defect-free, infinitely long shaft with the nominal diameter. The soil is assumed to be homogeneous. For this study, the Spectral-Analysis of Surface Waves (SASW) test results were used to calculate an average shear wave velocity in the upper 6 m (20 ft). Because there are no defects or shaft end to cause reflections, the theoretical mobility can only be the result of the initial impact and the reaction of the soil. The theoretical mobility plot for a 762-mm (30-in.) diameter, infinitely long shaft is shown in Figure 7. The experimental mobility curve is also plotted in Figure 7 for comparison. Because there are no reflections from defects or the end of the shaft, the portion of the theoretical curve from 200 to 1,000 Hz is free of the oscillations that are present in the experimental curve. The difference between the experimental curve and the theoretical curve is the desired result: a mobility plot that contains only the effect of reflections from defects and the end of the shaft.

$$\left(\frac{V(f)}{P(f)}\right)_{\text{Reflected}} = \left(\frac{V(f)}{P(f)}\right)_{\text{Experimental}} - \left(\frac{V(f)}{P(f)}\right)_{\text{Theoretical}} \quad (8)$$

The next step is to calculate the impulse response in the time domain by taking the inverse FFT of the "reflected" mobility. The result is a "relative reflectogram" that is a time history of the reflections that return to the top of the shaft. Next, the relative reflectogram is scaled to calculate the reflection coefficients corresponding to changes in impedance along the length of the shaft. With the reflection coefficients now determined, the impedance as a function of time is backcalculated using

$$Z(t) = Z(0) \cdot \exp\left[2 \cdot \int_0^t r(t)dt\right] \quad (9)$$

where

$Z(t)$ = impedance as a function of time,
$Z(0)$ = nominal impedance at the top of the shaft, and
$R(t)$ = reflection coefficients from the scaled relative reflectogram.

Finally, the impedance as a function of depth (the impedance log) is obtained from $Z(t)$ by converting time to depth using the compression wave velocity. As in the sonic mobility method, if the mass density and compression wave velocity are known, changes in impedance correspond to changes in the cross-sectional area or diameter of the shaft.

The impedance log for Shaft C2 is shown in Figure 8. The gray area in the figure is a vertical section through the shaft. The black rectangle is the nominal diameter and depth of the shaft. The impedance log underpredicts the length of the shaft by 1.2 m (3.9 ft). The impedance log also shows that the diameter of the shaft in the upper 5 m (16.4 ft) was close to the nominal diameter, 762 mm (30 in.). However, over the remaining 10 m (32.8 ft) of shaft, the impedance log shows that the actual diameter was larger than the nominal diameter.

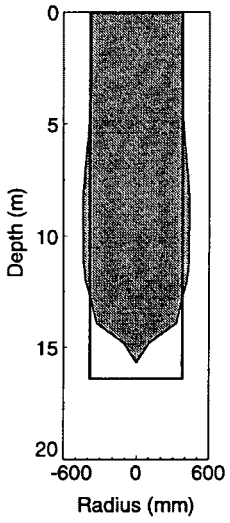


**FIGURE 8 Impedance log for Shaft C2.**

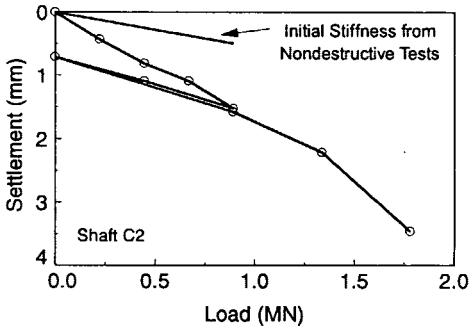


**FIGURE 9 Early portion of the load versus settlement curve for Shaft C2.**

The maximum diameter from the impedance log is 876 mm (34.5 in.). This enlargement is consistent with the concrete volumes used in Shaft C2. Field notes taken during construction of the shaft indicate that 6.9 $m^3$ (9 $yd^3$) of concrete was placed in the lower 11.4 m (37.4 ft) of the shaft. The average diameter of the shaft over this 11.4 m (37.4 ft) must then be 878 mm (34.6 in.). The agreement between the predicted diameter and actual average diameter is remarkable.

## COMPARISON OF TEST RESULTS

Static load tests were performed on Shafts C1 and C2. For both shafts, the load was increased to 0.89 MN (100 tons) in 0.22-MN (25-ton) increments. The shafts were unloaded and then reloaded to failure. Figure 9 shows the early portion of the load versus settlement curve for Shaft C2. The stiffness of the shaft for the initial loading part of the curve [0 to 0.89 MN (0 to 100 tons)] was 0.6 MN/mm (3,426 kips/in.). The stiffness associated with the unload-reload hysteresis loop was 1.0 MN/mm (5,882 kips/in.). Similar calculations for Shaft C1 yielded an initial stiffness of 0.5 MN/mm (2,941 kips/in.) and a stiffness of 1.2 MN/mm (6,666 kips/in.) from the unload-reload loop.

Tables 2 and 3 summarize the results of the nondestructive integrity tests and the static load tests. For Shaft C1 all of the methods underestimated the length of the shaft. The difference was particularly large for the impedance log method. A likely explanation is that the nondestructive methods were more sensitive to the impedance change associated with the socketing of the shaft into partially weathered rock at a depth of approximately 19.5 m (64 ft) than the end of the shaft. Similar results have been noted by others performing tests on socketed shafts (*4*). Two of the methods provide an estimate of the actual diameter of the shaft. The average diameter from the sonic mobility test was 851 mm (33.5 in.). The impedance log approach gives the diameter as a function of depth. Values ranged from 742 mm (29.2 in.) in the upper 5 m (16.4 ft) of the shaft to a maximum of 925 mm (36.4 in.) in the

**TABLE 2 Summary of Nondestructive and Static Load Tests for Shaft C1**

| Method | Length (m) | Diameter (mm) | Stiffness (MN/mm) |
|---|---|---|---|
| Sonic Echo | 17.3 | NA | NA |
| Sonic Mobility | 18.2 | 851 | 2.0 to 2.5 |
| Dynamic Impedance Function | NA | NA | 1.8 |
| Impedance Log | 14.9 | 742-925 | NA |
| Design/Actual | 21.4 | 762 | 0.5[a]<br>1.2[b] |

[a] from initial loading
[b] from unload-reload loop

**TABLE 3 Summary of Nondestructive and Static Load Tests for Shaft C2**

| Method | Length (m) | Diameter (mm) | Stiffness (MN/mm) |
|---|---|---|---|
| Sonic Echo | 17.5 | NA | NA |
| Sonic Mobility | 17.2 | 979 | 2.0 to 2.7 |
| Dynamic Impedance Function | NA | NA | 1.8 |
| Impedance Log | 15.7 | 740-876 | NA |
| Design/Actual | 16.9 | 762 | 0.6[a]<br>1.0[b] |

[a] from initial loading
[b] from unload-reload loop

lower 10 m (32.8 ft). As with Shaft C2, records made at the time or pouring indicate that 6.9 $m^3$ (9 $yd^3$) of concrete was placed in the lower 11.6 m (38 ft) of the shaft. This corresponds to an average diameter of 869 mm (34.2 in.) in the lower two-thirds of the shaft. The agreement between the diameter estimates from the two nondestructive tests and the independent calculation based on volume of concrete is excellent.

The low-strain stiffness from dynamic impedance function measurements are less than the sonic mobility stiffness by about 10 to 30 percent for Shaft C1. The difference is due to the inclusion of damping in $K_{mob}$. Both stiffnesses are larger than those measured during the initial loading and unload-reload portions of the static load test. The reason for the differences is the strain level associated with each stiffness. The nondestructive tests measure the stiffness at small strains ($<10^{-3}$ percent) where the soil surrounding the shaft behaves as a linear elastic material. The static load test involves larger displacements and strains with a corresponding decrease in the stiffness of the soil. Similar differences between the stiffnesses from nondestructive tests and static load tests have been noted elsewhere (*9*).

The results of the nondestructive tests on Shaft C2 have been presented in the previous section, but it is useful to summarize them here. The three methods that provide length estimates all yielded estimates that agree well with the design length. Both the sonic echo and sonic mobility approaches slightly overestimated the length; the impedance log underestimated the length by 7 percent. The impedance log accurately measured the variation in the diameter of Shaft C2 with depth. In the upper 5 m (16.4 ft) of the shaft, the 740-mm (29.1-in.) diameter is close to the nominal diameter and the enlarged diameter in the lower 10 m (32.8 ft) is consistent with the average diameter calculated using concrete volume. The average diameter of 979 mm (38.5 in.) from the sonic mobility test overestimates the apparent actual diameter of the shaft. Finally, the low-strain stiffnesses from the mobility and impedance function tests exceed the initial loading and unload-reload stiffnesses from the static load test as shown in Figure 9. The difference is caused by the difference in strain levels between the nondestructive tests and the static load tests.

It was mentioned earlier that the low-strain stiffnesses from nondestructive tests are frequently used as a relative measurement of foundation performance. The low-strain stiffnesses for Shaft C1 and C2 agree well. When used as a relative measurement, the low-strain stiffnesses accurately predicted that both Shafts C1 and C2 would have approximately the same static stiffness.

## CONCLUSIONS

Each of the four nondestructive methods has strengths and weaknesses. The sonic echo method is the simplest of the methods to perform and also the simplest to process and interpret. The method is limited in that only the length of the shaft and depths to defects can be determined. The sonic mobility approach requires more sophisticated, frequency domain processing and interpretation. However, its ability to determine the shaft length, depth of defects, average cross-sectional area, and low-strain stiffness makes it more versatile than the other methods. The dynamic impedance function approach provides only an estimate of the low-strain stiffness of the shaft. However, the value of stiffness more accurately reflects the true low-strain static stiffness because the influence of damping is excluded from the definition of stiffness. The strength of the impedance log is in its ability to determine the variation of a cross-sectional area or diameter along the length of the shaft. The ability to produce a "picture" of a vertical section through the shaft is the most persuasive form of output from the four test methods.

It is important to note that all four methods complement one another. Acquisition of data in the field is the same for each method. The differences are in the way the data are processed and interpreted. It is possible, therefore, to use more than one method to complement and/or confirm the results without the need for different field test procedures or equipment.

The ability to use several of these methods to complement one another becomes particularly important if nondestructive methods are used for the unknown foundation problem. In these cases, the interpretation of test results may be more difficult due to the deterioration of the shaft. The impedance log is valuable because it produces the most complete visual representation of the shaft. The low-strain axial stiffness from either the sonic mobility or the dynamic impedance function approach is a measure of the performance of the shaft under load. The stiffness value is potentially useful in rapidly and nondestructively assessing the ability of a deteriorated shaft to carry additional load.

## ACKNOWLEDGMENTS

The authors wish to thank the following organizations for their participation and support of the load test program: ASCE Georgia Section Geotechnical Committee, ATEC Associates, Atlanta Testing and Engineering, Brainard Kilman, Inc., Case International, Dames and Moore, Georgia Department of Transportation, Georgia Tech's Office of Facilities, Geo-Syntec Consultants, Golder Associates, Johnson Drilling Co., Law Engineering, Long Foundation Drilling Co., McKinney Drilling Co., Russo Corporation, Tensar Corporation, and Turner Engineering Consultants. The financial support of the Federal Highway Administration is also gratefully acknowledged.

## REFERENCES

1. Harris, D. *Load Tests of Two Drilled Shafts Constructed in Piedmont Residuum*. Master's thesis. Georgia Institute of Technology, 1992.
2. Hearne, T. M., K. H. Stokoe II, and L. C. Reese. Drilled Shaft Integrity by Wave Propagation Method. *Journal of Geotechnical Engineering*, ASCE, Vol. 107, No. GT10, Oct. 1981, pp. 1327–1344.
3. Stain, R. T. Integrity Testing. *Civil Engineering*, April 1982, pp. 54–59.
4. Olson, L. D., and C. C. Wright. Nondestructive Testing of Deep Foundations with Sonic Methods. *Foundation Engineering: Current Principles and Practices*, ASCE, Vol. 2, 1989, pp. 1173–1183.
5. Paquet, J. Étude Vibratoire Des Pieux En Béton, Réponse Harmonique Et Impulsionelle: Application Au Controle (in French).

*Annalles de l'Institut Technique du Batiment et des Travaux Publics*, No. 245, May 1968, pp. 788–803.
6. Gazetas, G. Analysis of Machine Foundation Vibrations: State of the Art. *Soil Dynamics and Earthquake Engineering*, Vol. 2, No. 1, 1983, pp. 2–42.
7. Novak, M. Piles Under Dynamic Loads. *Proc., Second International Conference on Recent Advances in Geotechnical Earthquake Engineering and Soil Dynamics*, St. Louis, Vol. 3, March 1991, pp. 2433–2456.
8. Paquet, J. A New Method for Testing Integrity of Piles by Dynamic Impulse: The Impedance Log (in French). *International Colloquium on Deep Foundations*, Paris, March 1991, pp. 1–10.
9. Baker, Jr., C. N., E. D. Drumwright, F. Menash, G. Parikh, and C. Ealy. Dynamic Testing to Predict Static Performance of Drilled Shafts: Results of FHWA Research. *Geotechnical Engineering Congress 1991*. Geotechnical Special Publication No. 27, ASCE, Vol. 1, 1991, pp. 491–504.

*Publication of this paper sponsored by Committee on Soil and Rock Properties.*